Published OnlineFirst June 10, 2011; DOI: 10.1158/1541-7786.MCR-10-0457

Angiogenesis, Metastasis, and the Cellular Microenvironment

Molecular Cancer Research

Notch1 Inhibition Alters the CD44^{hi}/CD24^{lo} Population and Reduces the Formation of Brain Metastases from Breast Cancer

Patricia M. McGowan[1], Carmen Simedrea[1], Emeline J. Ribot[4], Paula J. Foster[1,4], Diane Palmieri[5], Patricia S. Steeg[5], Alison L. Allan[2,3], and Ann F. Chambers[1,2]

Abstract

Brain metastasis from breast cancer is an increasingly important clinical problem. Here we assessed the role of CD44^{hi}/CD24^{lo} cells and pathways that regulate them, in an experimental model of brain metastasis. Notch signaling (mediated by γ-secretase) has been shown to contribute to maintenance of the cancer stem cell (CSC) phenotype. Cells sorted for a reduced stem-like phenotype had a reduced ability to form brain metastases compared with unsorted or CD44^{hi}/CD24^{lo} cells ($P < 0.05$; Kruskal–Wallis). To assess the effect of γ-secretase inhibition, cells were cultured with DAPT and the CD44/CD24 phenotypes quantified. 231-BR cells with a CD44^{hi}/CD24^{lo} phenotype was reduced by about 15% in cells treated with DAPT compared with DMSO-treated or untreated cells ($P = 0.001$, ANOVA). *In vivo*, mice treated with DAPT developed significantly fewer micro- and macrometastases compared with vehicle treated or untreated mice ($P = 0.011$, Kruskal–Wallis). Notch1 knockdown reduced the expression of CD44^{hi}/CD24^{lo} phenotype by about 20%. *In vitro*, Notch1 shRNA resulted in a reduction in cellular growth at 24, 48, and 72 hours time points ($P = 0.033$, $P = 0.002$, and $P = 0.009$, ANOVA) and about 60% reduction in Matrigel invasion was observed ($P < 0.001$, ANOVA). Cells transfected with shNotch1 formed significantly fewer macrometastases and micrometastases compared with scrambled shRNA or untransfected cells ($P < 0.001$; Kruskal–Wallis). These data suggest that the CSC phenotype contributes to the development of brain metastases from breast cancer, and this may arise in part from increased Notch activity. *Mol Cancer Res; 9(7); 834–44. ©2011 AACR.*

Introduction

Brain metastasis from breast cancer is a growing problem, due in part to improved therapies for systemic metastatic disease and the inability of many conventional drugs to cross the blood-brain barrier. Ten to 16% patients with metastatic breast cancer historically developed brain metastases, with a 1 year survival of 20% (1–2). Currently, one-third of metastatic breast cancer patients with either HER2 positive tumors or "triple negative" tumors (estrogen and progesterone receptor negative, HER2 normal) develop brain metastases (1, 3–6). In addition, much remains to be elucidated about the mechanisms involved in the formation of brain metastases from breast cancer, and the processes by which it is regulated. It is hoped that such information, combined with improved blood-brain barrier pharmacokinetics, will enable the identification and validation of novel therapeutics with increased potency in the brain (for review, ref. 7). Here we investigated the role of the cancer stem cell (CSC) phenotype and, in particular, the Notch pathway, in an experimental model of breast cancer metastasis to the brain.

Stem cells are defined as cells that have the ability to (i) sustain themselves through self-renewal and (ii) generate mature cells through differentiation (8). Growing evidence suggests that CSCs have similar self-renewal capacity to that of normal stem cells, and that only a subset of tumor cells have the ability to grow and divide to repopulate a tumor. As such, the identification and study of these cells, in addition to the pathways that regulate their maintenance, may allow selective targeting of the core population of tumor promoting cells. In breast cancer, Al-Hajj and colleagues identified a population of CD44^{+}CD24$^{-/lo}$Lineage^{-} cells in breast cancer patients (9). As few as 100 cells with this phenotype were able to initiate and form a tumor *in vivo*. In contrast, 20,000 cells with alternate phenotypes were unable to form tumors (9). In addition, measurement of aldehyde dehydrogenase (ALDH) activity has recently been utilized to

Authors' Affiliations: Departments of [1]Medical Biophysics, [2]Oncology and [3]Anatomy and Cell Biology; [4]Robarts Research Institute, University of Western Ontario, London, Ontario, Canada; and [5]Women's Cancers Section, Laboratory of Molecular Pharmacology, Center for Cancer Research, National Cancer Institute, Bethesda, Maryland

Note: Supplementary data for this article are available at Molecular Cancer Research Online (http://mcr.aacrjournals.org/).

Corresponding Author: Patricia M. McGowan, Education and Research Centre, St. Vincent's University Hospital, Elm Park, Dublin 4, Ireland. Phone: 353-1-221-4772; Fax: 353-1-221-4428; E-mail: patricia.mcgowan@ucd.ie

doi: 10.1158/1541-7786.MCR-10-0457

Published OnlineFirst June 10, 2011; DOI: 10.1158/1541-7786.MCR-10-0457

identify normal stem cells and CSCs (10, 11). ALDH1 levels have been found to correlate with high tumor grade, HER2 positivity, hormone receptor negativity and expression of the basal markers cytokeratin (CK) 5/6 and CK14 (12). In addition, expression of ALDH1 was shown to be an independent prognostic indicator of poor overall survival for breast cancer. Increasing evidence suggests that CSCs play an important role in mediating metastasis. Indeed ALDH-positive breast cancer cell lines showed enhanced metastatic capabilities when injected into NOD/SCID mice (13).

Notch proteins are a family of 4 transmembrane, heterodimeric receptors (Notch1IC–Notch4IC), with 5 known ligands (Delta-like1, Delta-like3, Delta-like4, Jagged1 and Jagged2). In response to ligand binding, the intracellular domain of the receptor is proteolytically released in 2 stages, mediated by ADAM proteases (14, 15) and a γ-secretase [presenilin; (16)]. The cleaved intracellular domain translocates to the nucleus where it is involved in transcriptional activation of the CSL (CBF1-Suppressor of Hairless-Lag2) transcription factor family. Following Notch binding to CSL, it becomes a transcriptional activator. In combination with Mastermind-like (MAML) proteins, transcriptional induction of Hairy/Enhancer of Split genes occurs, for example, Hey, Hes, and Notch1 itself. Elevated Notch signaling has also been found to increase transcription of HER2 (17) and cyclin D1 (18), among others.

Dysregulated Notch signaling has been observed in many human cancers, including endometrial cancer (19), colon cancer (20), and lung cancer (21). Recently, it has been shown that Notch signaling is activated in human breast cancer, with the accumulation of Notch1 intracellular domain in tissue (22). Notch signaling in breast cancer has also been shown to activate Akt (23) and survivin (24), which may be involved in mediating chemoresistance. Elevated Notch ligands have been shown to correlate with poor overall survival in patients with breast cancer (25). Notch signaling has previously been shown to play a role in stem cell maintenance (26, 27), and may also contribute to the maintenance of the CSC phenotype (28–31), with the strongest evidence for a role in CSCs being in breast cancer. Gamma-secretase inhibition has been shown to prevent the formation of secondary mammospheres from cell lines and primary patient samples (32). A role for CSC in metastasis has been proposed but remains incompletely defined (33–35). Similarly, a role for the Notch pathway in tumor metastasis has been proposed (36–39). Nam and colleagues reported that a MDA-MB-435 carcinoma cell line selected for metastatic growth in the brain exhibited upregulation of the Notch pathway as compared with the parental cell line, and that the commercial γ-secretase inhibitor DAPT and RNA interference-mediated knockdown of Notch1 inhibited tumor cell migration and invasion *in vitro* (40).

In this study, we used an experimental model of brain metastasis of breast cancer to assess the role of the Notch pathway in brain metastases of breast cancer *in vivo*. Using two different experimental strategies, Notch signaling inhibition significantly prevented the colonization of brain metastatic MDA-MB-231 (231-BR) human breast cancer cells in the brain. We also determined the relationship of the "stem-like" phenotype ($CD44^{hi}/CD24^{lo}$) to both brain metastasis and Notch signaling inhibition. The data nominate Notch as a potential therapeutic target for inhibition of brain metastases.

Materials and Methods

Cell culture

MDA-MB-231 (231) human breast carcinoma cells (American Type Culture Collection) and the brain metastatic variant 231-BR cells (41) were maintained in Dulbecco's-minimal essential media (DMEM; Invitrogen), supplemented with 10% FBS (Sigma Aldrich).

Cell surface marker analysis

231, 231-BR, 231-BR-shNotch1, 231-BR-shScrambled cells and cells treated with 5 μmol/L DAPT [*N*-(*N*-(3,5-difluorophenacetyl)-L-alanyl)-*S*-phenylglycine *t*-butyl ester (Sigma Aldrich)] or DMSO (dimethyl sulfoxide; Sigma; 1×10^5) were incubated with fluorescently conjugated antibodies, including anti-CD24 (clone ML5; BD Biosciences) conjugated to phycoerytherin (PE); and anti-CD44 (clone IM7; BD Biosciences) conjugated to fluorescein isothiocyanate (FITC). Fluorescently conjugated IgG isotype controls (BD Biosciences) were used as negative controls. Cells were analyzed using a Beckman Coulter EPICS XL-MCL flow cytometer (Beckman Coulter). Data are illustrated as percentage of cells with a $CD44^{hi}/CD24^{lo}$ phenotype (bottom right quadrant) ± SE.

Fluorescence-activated cell sorting (FACS)

231-BR cells were labeled with fluorescent antibodies (CD44-FITC + CD24-PE). Cell subsets were isolated using a 4-color analysis protocol on a FACS Vantage/Diva cell sorter (BD Biosciences), into $CD44^{hi}CD24^{lo}$ (defined as "stem like") and $CD44^{lo}CD24^{hi}$ ("nonstem like") subsets (top and bottom 5%). Cell viability was assessed by plating efficiency postsorting. Following FACS isolation, cells were used immediately for *in vivo* assays. Sorting was conducted at the Robarts Research Institute Flow Cytometry facility, University of Western Ontario.

Analysis of ALDH activity

To assess ALDH activity of the different cell lines, the Aldefluor assay kit (StemCell Technologies) was used. The basis for this assay is that uncharged ALDH substrate [BODIPY-aminoacetaldehyde (BAAA)] is taken up by living cells *via* passive diffusion. Once inside the cell, BAAA is converted into negatively charged BODIPY-aminoacetate (BAA−) by intracellular ALDH. BAA− is then retained inside the cell, causing the cell to become highly fluorescent. Only cells with an intact cell membrane can retain BAA−, so only viable cells can be identified (13). The Aldefluor assay was conducted essentially as described previously (10, 11). Briefly, 231-BR cells were harvested, placed in Aldefluor assay buffer (2×10^6 cells/mL), and incubated with the Aldefluor substrate for 45 minutes at 37°C to allow

Published OnlineFirst June 10, 2011; DOI: 10.1158/1541-7786.MCR-10-0457

substrate conversion. As a negative control for all experiments, an aliquot of Aldefluor-stained cells was immediately quenched with 1.5-mmol/L diethylaminobenzaldehyde (DEAB), a specific ALDH1 inhibitor. Cells were analyzed using the green fluorescence channel (FL1) on a Beckman Coulter EPICS XL-MCL flow cytometer.

In vivo brain metastasis assays

All *in vivo* work was carried out using 6 to 7 week old female athymic nude nu/nu mice (Charles River Laboratories). Animal procedures were conducted in accordance with the recommendations of the Canadian Council on Animal Care, under a protocol approved by the University of Western Ontario Council on Animal Care. Cells were grown to about 75% confluency in 75 cm^2 flasks. Following cell sorting, sorted populations ($CD44^{hi}CD24^{lo}$ and $CD44^{lo}CD24^{hi}$ 231-BR cells) were resuspended in sterile Hank's buffered salt solution (HBSS, Invitrogen) at 1.75×10^5 cells/0.1 mL. Mice were anaesthetized with isofluorane/O_2 and cells were injected into the left ventricle, as described previously (42). Similarly, 231-BR cells transfected with shNotch1 or shScrambled were injected intracardiac at 1.75×10^5 cells/mouse. For γ-secretase inhibition study, we used a commercially available γ-secretase inhibitor, DAPT (Sigma Aldrich). Following injection of 1.75×10^5 231-BR cells, tumors were allowed to form for 14 days. Mice were treated intraperitoneally with 8 mg/kg DAPT (or vehicle: 5% ethanol in corn oil), beginning treatment on day 14 using a 3-day on, 4-day off schedule up to day 28. Intermittent administration of DAPT has previously been shown to reduce the gastrointestinal toxicity observed with γ-secretase inhibition which can result from expansion of goblet cells (43, 44). Mice were euthanized on day 28 and the whole brains were removed from the skull and assessed for metastatic growth. Brains were fixed in formalin, embedded in paraffin and sectioned (10 μm sections). Sections were stained using standard hematoxylin and eosin (H&E) staining. The number of metastases per section was determined by light microscopy, by 2 independent blinded investigators. Metastases were binned into micro- and macrometastases using 50 μm^2 as a cut-off, as described previously (42).

RNA isolation and real-time PCR

RNA from cell lines was isolated using the RNeasy Mini kit (Qiagen). All RNA was reverse transcribed using SuperScript III reverse transcriptase (Invitrogen). Primers were obtained for Notch 1 to 4, Hey1, and 18S (SABiosciences). The optimized amplification protocol consisted of an initial denaturation step of 95°C for 10 minutes followed by 36 amplification cycles at 95°C for 10 seconds, annealing at 58°C for 5 seconds, and elongation at 72°C for 10 seconds. A constant temperature ramp of 20°C/second was used throughout each of the steps. Measurements of fluorescence were taken at the end of the annealing phase for each cycle. The PCR products were melted by increasing the temperature to 95°C (0.1°C/second). Finally, the samples were cooled to 40°C. Real-time PCR (RT-PCR) was conducted using the CFX96 Real-Time PCR Detection System (Bio-Rad Laboratories). As a negative control, cDNA was replaced with deionized water. To quantify gene expression, the internal control transcript 18S rRNA was used as a reference. Data were analyzed using the Pfaffl method (45) and is displayed as fold changes relative to control cells.

Immunoblotting

Protein was extracted from cell lines using RIPA (radioimmunoprecipitation assay) buffer containing protease inhibitors (EDTA-free-Protease inhibitor cocktail; Roche). Protein concentrations were measured using the Nanodrop spectrophotometer (Nanodrop 2000, Thermo Scientific, Rockford). A total of 100 μg of protein were separated on SDS-PAGE and transferred to PVDF (polyvinylidene fluoride) membranes. Membranes were blocked in 5% low fat milk solution in TBS-T (Tris-buffered saline with 0.05% Triton X100) for 1 hour at room temperature, and then incubated overnight with primary antibody [1:1,000 cleaved Notch1: Cell Signaling Danvers; 1: 10,000 GAPDH (Glyceraldehyde 3-phosphate dehydrogenase): Sigma]. Following 3 washes for 10 minutes in TBS-T, the membrane was incubated with 1:1,000 HRP (horseradish peroxidase)-conjugated anti-rabbit Ig secondary antibody (Sigma) for 2 hours at room temperature. Antibody binding was detected using enhanced chemiluminescence (Thermo Scientific) and visualization using ChemiDoc XRS+ System (Bio-Rad Laboratories).

Transfection of 231-BR cells with Notch1 shRNA

Cells were transiently transfected with a pool of 4 predesigned Notch1 shRNA vectors or a scrambled vector (SureSilencing, SABiosciences), according to the manufacturer's instructions (for sequences, see Supplementary Table S1). 231-BR cells were transfected using the Lonza nucleofection technology (Lonza). Briefly, 1×10^6 231-BR cells were resuspended in Cell Line Nucleofector Kit V (Lonza), mixed with 2 μg cDNA and pulsed with the program X-13, as suggested by the manufacturer. Immediately after nucleofection, cells were transferred into wells containing prewarmed (37°C) culture medium. Silencing of Notch1 expression was confirmed by RT-PCR.

Cell proliferation assay

231-BR, scrambled shRNA and Notch1 shRNA-transfected cells were plated at a density of 5×10^4 cells per well in 10 mm dishes in DMEM plus 10% FBS ($n = 3$/timepoint). Every 24 hours, for 3 days, triplicate cultures were trypsinized and counted by hemocytometer.

Cell invasion assay

231-BR, scrambled shRNA and Notch1 shRNA-transfected cells (2.5×10^4 cells/well), in DMEM containing 10% FBS, were seeded in the upper compartment of Matrigel-coated inserts (24-well plate, 8 μmol/L pore size; BD Biocoat, BD Biosciences). The lower chamber was filled with DMEM with 25% FBS. After 24 hours of incubation at 37°C, nonmigrated cells in the upper chamber were

Published OnlineFirst June 10, 2011; DOI: 10.1158/1541-7786.MCR-10-0457

removed from the upper surface of the filters using a phosphate buffered saline (PBS)-soaked cotton swab. This was followed by fixation in 1% glutaraldehyde and staining with 0.1% crystal violet. Cells fixed on the lower face of the Matrigel chambers were counted under a light microscope. Five high-powered fields were counted for each well and mean numbers of invaded cells per field were counted. All experiments were carried out in duplicate, using 2 independent assays.

Data analysis

In vivo experiments with FACS-sorted cells were carried out three times, with data pooled from all 3 (Control, unsorted cells: $n = 7$, $CD44^{hi}/CD24^{lo}$ cells: $n = 5$, $CD44^{lo}/CD24^{hi}$ cells: $n = 10$). shNotch1 *in vivo* experiments were conducted once (Control, untreated: $n = 7$, 231-BR-shScrambled injections: $n = 9$, 231-BR-shNotch1 injections: $n = 7$). DAPT treatments were conducted once (Untreated mice: $n = 10$, Vehicle-treated mice: $n = 9$, 8 mg/kg DAPT-treated mice: $n = 10$). Statistical analysis was conducted using SPSS statistics version 15.0 (SPSS Inc.). Differences between means were determined using the Kruskal–Wallis (for *in vivo* data), ANOVA or Student's paired *t* test (for *in vitro* data) tests. Data are presented as the mean ± SEM.

Analysis of a published microarray data set

We interrogated a comprehensive gene expression microarray data set of 295 primary breast tumors (obtained from Rosetta Inpharmatics) prepared by van de Vijver and colleagues, who used it to identify gene expression signatures predictive of outcome. The detailed clinical characteristics of these tumors have been previously published (46). Univariate relationships between Notch mRNA log ratio data and patient outcome were assessed using the Log-rank test (RR, CI). A RR of 1 indicates that the risk of relapsing or dying is the same in both groups, while a RR of more than 1 indicates an increased risk of relapse or death. CIs were calculated for the RR, which was then tested for statistical significance using the Wald test. Data were assigned arbitrary cutoff points of 25th, 50th, and 75th percentiles, with the 75th percentile yielding the most interesting results. Data are presented using Kaplan–Meier curves. $P \leq 0.05$ were regarded as being statistically significant. As above, data were analyzed using SPSS statistics version 15.0 (SPSS Inc.).

Results

Characterization of CSC properties of 231-BR cells

MDA-MB-231 parental breast cancer cells have been shown to have little or no metastatic growth to the brain *in vivo* (41). The 231-BR cell line model used in this study has been selected *in vivo* for increased brain metastatic ability (40). Previous work reported that parental MDA-MB-231 cells had approximately 80% cells with a $CD44^{hi}/CD24^{lo}$ phenotype (13). The proportion of $CD44^{hi}/CD24^{lo}$ cells in brain metastatic 231-BR cells was compared with parental 231 cells by flow cytometry. We found that 231 cells were 92.12% $CD44^{hi}/CD24^{lo}$ and the 231-BR cells were 90.68% $CD44^{hi}/CD24^{lo}$ (Fig. 1A). Previous work also showed that a distinct subgroup of 231 parental cells displayed increased ALDH activity, another marker of potential CSC function (13). However, upon analysis of 231-BR cells, a uniform, whole population increase in ALDH activity was observed (Fig. 1B), which did not reach statistical significance and was therefore not suitable, in this investigation, for use as an additional enrichment factor.

To continue our investigation into the CSC phenotype in brain metastases, FACS was used to isolate subsets of cells from 231-BR cells using $CD44^{hi}/CD24^{lo}$ expression as the primary sort criteria. The resulting cell subsets were designated as $CD44^{hi}/CD24^{lo}$ (stem-like, referred to as CSC) and $CD44^{lo}/CD24^{hi}$ (nonstem-like, referred to as non-CSC). $CD44^{hi}/CD24^{lo}$ cells (average of 99.49% population purity following cell sorting) and $CD44^{lo}/CD24^{hi}$ (average of 95.4% purity) sorted cells. The sorted cells, as well as unsorted 231-BR cells (which are 90.68% $CD44^{hi}/CD24^{lo}$), were injected by the intracardiac route into nude mice, as described previously (42), and allowed to form tumors for 28 days (Table 1). On day 28, mice were sacrificed and brains were removed, formalin fixed and paraffin embedded. The incidence and numbers of micro- and macrometastases were determined by histology (data presented as an average of 3 sections/mouse), by 2 independent observers using an ocular micrometer. Representative H&E stained images can be seen in Supplementary Figure S1. 231-BR cells with a $CD44^{lo}/CD24^{hi}$ non-CSC phenotype formed a mean of 44.5 ± 9.5 micrometastases and 16.2 ± 3.6 macrometastases per histologic section. This represented a 25% and 45% reduction, respectively, compared with brain metastasis formation by 231-BR cells with a $CD44^{hi}/CD24^{lo}$ CSC phenotype, which produced 59.4 ± 17.8 micrometastases and 29.9 ± 10.2 macrometastases per section. The formation of both micro- and macrometastases was statistically significantly different in the 2 sorted populations (micrometastases: $P < 0.0001$; macrometastases: $P = 0.02$, Kruskal–Wallis test). Thus, the cells sorted for a reduced stem-like phenotype had a reduced ability to form brain metastases. The number of metastases formed in the $CD44^{lo}/CD24^{hi}$ experimental group is likely due to the reduced purity of the population obtained following cell sorting or the uniform expression of ALDH observed in the entire cell population (Fig. 1B). In addition, it is important to note that the phenotype of CD44hi/CD24lo is a dynamic one and the population tends to return to baseline at approximately 7 days postsorting (data not shown).

Role of Notch pathway in breast cancer aggressiveness and the CSC phenotype of 231-BR cells

Due to the reported role of Notch signaling in the maintenance of the CSC phenotype (28–30), the role of Notch signaling in the 231-BR model was studied. The levels of Notch 1 to 4 mRNA in 231 and 231-BR cells were determined by RT-PCR. Both 231 and 231-BR cell lines

Published OnlineFirst June 10, 2011; DOI: 10.1158/1541-7786.MCR-10-0457

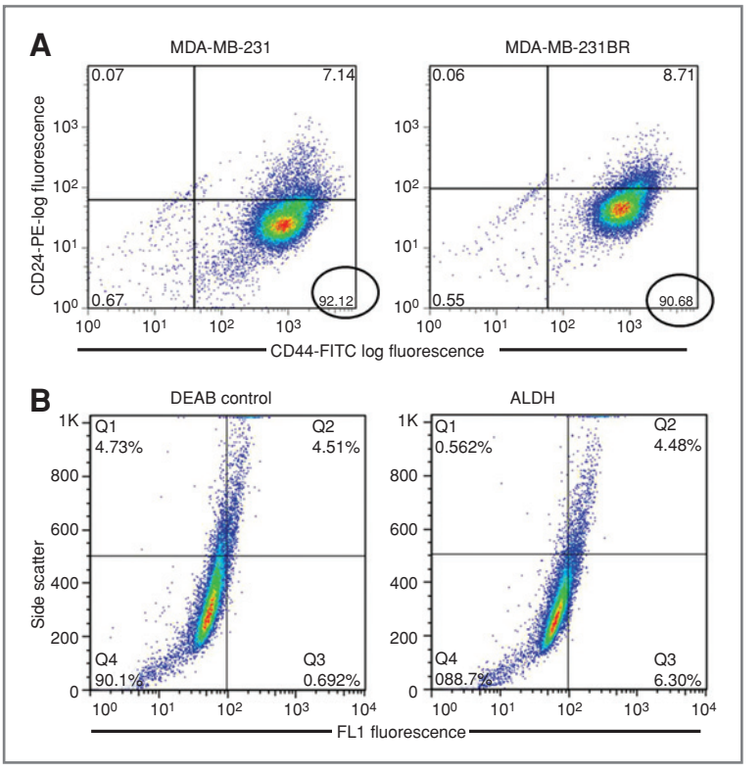

Figure 1. A, flow cytometric analysis of CD44/CD24 cell surface markers. Antibodies used included an anti-CD44 antibody (clone IM7) conjugated to FITC, an anti-CD24 antibody (clone ML5) conjugated to PE, (appropriate FITC- and PE-conjugated IgG isotype controls were also included, data not shown). On the left, representative dot plots of CD44-FITC versus CD24-PE expression for MDA-MB-231 parental cells is shown. On the right, representative dot plot of CD44-FITC versus CD24-PE expression for 231-BR cells is shown. For cells which fell in the bottom right hand quadrant (percentages circled), we considered to express the CSC phenotype of interest ($CD44^{hi}/CD24^{lo}$). B, flow cytometric analysis of ALDH activity in 231-BR cells. Cells were analyzed using the Aldefluor assay kit (StemCell Technologies), according to the manufacturer's instructions. As a negative control, an aliquot of Aldefluor-stained cells was immediately quenched with 1.5 mmol/L DEAB, a specific ALDH1 inhibitor, was included as a negative control. Cells were analyzed using the green fluorescence channel (FL1) on a BD FACSCalibur cytometer. On the left, a representative dot plot of cells treated with DEAB, the ALDH inhibitor is shown. On the right, a representative dot plot of ALDH activity is shown.

expressed Notch 1 to 4 mRNA at similar levels, relative to 18S rRNA (Fig. 2A), with no statistical differences observed. To extend our investigation, we analyzed a published database from the Netherlands Cancer Institute (295 consecutive primary breast cancer patients; ref 46). We found that elevated levels (>75th percentile) of Notch1 mRNA were associated with poor overall survival in patients with primary breast carcinoma (Fig. 2B), confirming a

Table 1. *In vivo* analysis of the effect of sorting for $CD44^{hi}/CD24^{lo}$ and $CD44^{lo}/CD24^{hi}$ on the formation of brain metastases compared with unsorted 231-BR cells

Group	Incidence	Mean micrometastases (median: range)	Mean macrometastases (median: range)
Unsorted 231-BR	7/11	73.3 (70.5: 44–135)	27.7 (20: 2–48)
$CD44^{hi}/CD24^{lo}$	5/9	59.4 (65: 28–119)	29.9 (30: 8–54)
$CD44^{lo}/CD24^{hi}$	10/10	44.5 (50: 8–79)[a]	16.2 (17: 1–29)[b]

NOTE: Data shown were pooled from 3 independent experiments. 1.75×10^5 cells (sorted and unsorted) were injected in nude mice via the intracardiac route. Mice were sacrificed 28 days later and brains were removed for histological analysis. Numbers shown are average values from 3 sections per mouse (median value and range also displayed). $CD44^{lo}/CD24^{hi}$ formed fewer micro- and macrometastases when compared with $CD44^{hi}/CD24^{lo}$ or unsorted 231-BR cells. Data were analyzed using Kruskal–Wallis test.
[a]$P < 0.05$.
[b]$P < 0.001$.

Published OnlineFirst June 10, 2011; DOI: 10.1158/1541-7786.MCR-10-0457

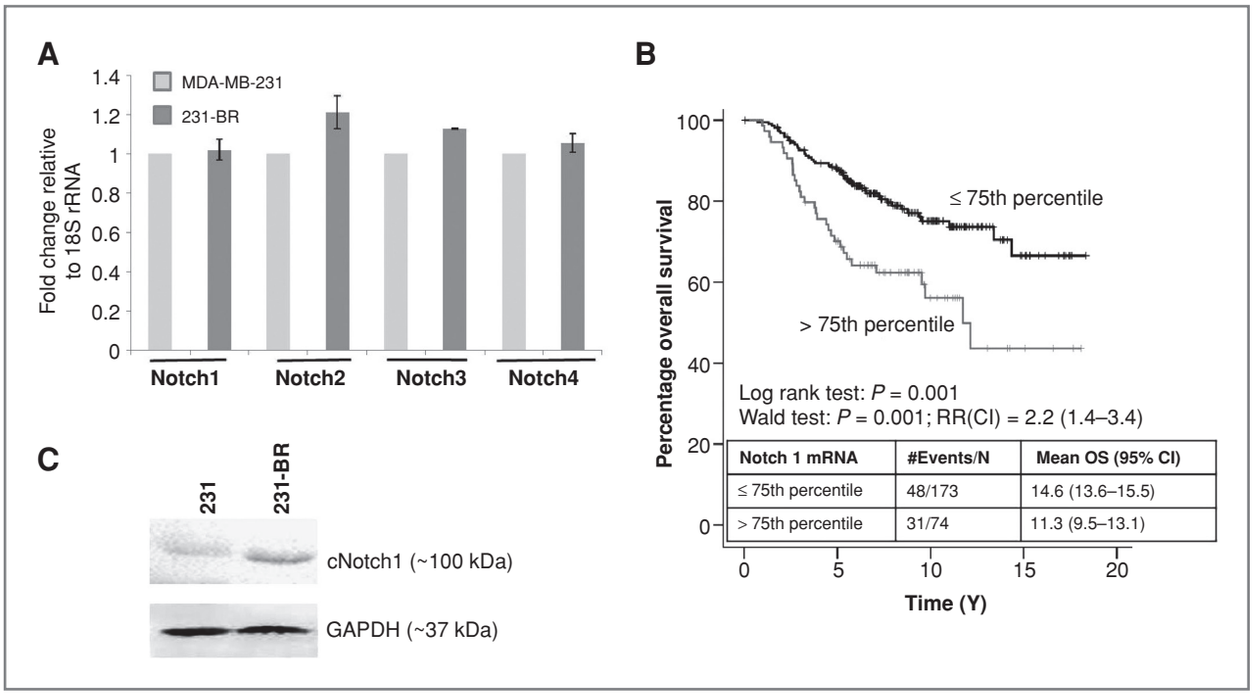

Figure 2. A, Notch 1 to 4 mRNA was measured in MDA-MB-231 parental cells (231) and 231-BR cells. There were no significant differences in mRNA expression. B, elevated levels of Notch 1 (>75th percentile) were associated with a significantly shorter overall survival. Univariate relationships between Notch mRNA log ratio data, from a publicly available database of 295 consecutive breast cancer patients, and patient outcome were assessed using the Log Rank test. CIs were calculated for the RR, which was then tested for statistical significance using the Wald test. Data were assigned arbitrary cutoff points of 25th, 50th, and 75th percentiles, with the 75th percentile yielding the most interesting results. Data are presented using Kaplan–Meier curves. No significant relationships were observed with Notch 2, 3, or 4. C, Cleaved Notch1IC protein was elevated in 231-BR cells compared with parental MDA-MB-231 cells.

potential role for elevated Notch1 in breast cancer aggressiveness. No significant relationships were observed with Notch 2 to 4 in this data set. Based on these observations, we pursued Notch1 as a target for further study. Levels of cleaved Notch1 protein (NICD, Notch 1 intracellular domain, cleaved by γ-secretase) were increased in 231-BR cells compared with 231 parental cells (Fig. 2C), as determined by Western blotting. The data indicate that the Notch pathway is expressed, and that intracellular cleavage of Notch 1 is elevated in 231-BR cells.

We then asked whether inhibition of the Notch pathway would alter the CSC phenotype of 231-BR cells. A commercial inhibitor of γ-secretase, DAPT, was utilized. To test the activity of DAPT on the 231-BR cell line, cells were cultured in 5 μmol/L DMSO ± 5 μmol/L DAPT for 24 hours, and the mRNA levels of Notch pathway members were quantified by RT-PCR. Reductions in Notch 1 to 4 mRNA levels (Fig. 3A) were observed in response to DAPT treatment, with reductions in Notch 1, 3, and 4 reaching statistical significance.

To ask if Notch inhibition influenced the stem cell phenotype of 231-BR cells *in vitro*, cells were cultured in DMSO ± DAPT and the CD44/CD24 phenotypes quantified. Flow cytometric analysis revealed that the percentage of 231-BR cells with a $CD44^{hi}/CD24^{lo}$ CSC phenotype was reduced by about 15% (from ~92% to ~75%) in cells treated with 5 μmol/L DAPT for 24 hours compared with DMSO-treated or untreated cells ($P = 0.001$, ANOVA; Fig. 3B). This was accompanied by a parallel increase in $CD44^{hi}/CD24^{hi}$ markers from ~7% to ~24%). The effect of DAPT on 231-BR proliferation *in vitro* was assessed using a growth curve assay (Fig. 3C). While vehicle had no significant effect on 231-BR proliferation, 5 μmol/L DAPT reduced proliferation by 54.2% and 45.1% at 24 and 48 hours of culture ($P = 0.023$, $P < 0.0001$, respectively; ANOVA). In addition, treatment of 231-BR cells with 5 μmol/L DAPT *in vitro* resulted in a significant reduction in mRNA levels of downstream transcriptional target Hey1 (Supplementary Fig. S2A). The data indicate that DAPT, a Notch inhibitor, reduced the stem cell phenotype of 231-BR cells *in vitro* with a resulting anti-proliferative effect.

Effect of Notch inhibition on 231-BR brain metastasis *in vivo*

Extending our findings from the *in vitro* setting, we examined the effect of γ-secretase inhibition, using DAPT, *in vivo*. 231-BR cells were injected into the left cardiac ventricle of immunodeficient mice, and mice were randomized to vehicle or 8 mg/kg (3 days on, 4 days off

Published OnlineFirst June 10, 2011; DOI: 10.1158/1541-7786.MCR-10-0457

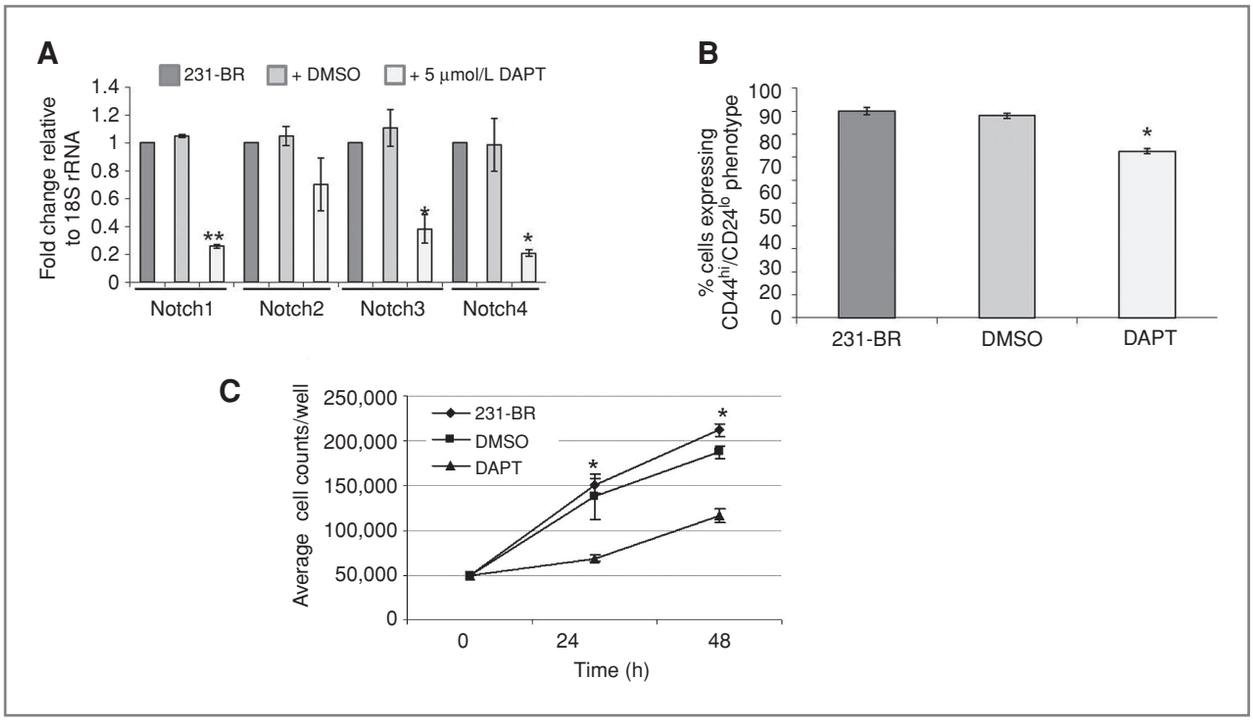

Figure 3. Effect of γ-secretase inhibition using DAPT (Sigma) on *in vitro* cellular behavior. A, DAPT treatment reduced the expression of Notch 1, 2, 3, and 4 mRNA, $P < 0.01$, ANOVA (*, $P < 0.05$, **, $P < 0.001$, Student's paired *t* test DAPT compared with DMSO). B, CSCs markers, CD44 and CD24 were determined in 231-BR, DMSO-treated and 5 μmol/L DAPT-treated cells. DAPT reduced the percentage of $CD44^{hi}/CD24^{lo}$ cells, compared with IgG controls, by approximately 15% compared with untreated or DMSO-treated control cells ($P = 0.001$, ANOVA; $P < 0.05$ DAPT compared with DMSO control, Student's paired *t* test). C, DAPT treatment resulted in a significant reduction in cellular growth at 24 and 48 hours (*, $P = 0.023$, $P < 0.001$, respectively, ANOVA).

schedule) DAPT beginning on day 14 postinjection. On day 28, mice were sacrificed and brains were removed, formalin fixed and paraffin embedded. Micro- and macrometastases were counted by 2 independent observers on 3 H&E stained sections per brain, using an ocular micrometer (Table 2), as previously described (42). Mice treated with DAPT developed a mean of 26.1 ± 5.9 macrometastases per section, 25% lower than vehicle-treated (34.9 ± 2.4 per section) or untreated (34.6 ± 2.4 per section) mice ($P = 0.011$, Kruskal–Wallis test). A similar reduction in micrometastases was observed for DAPT-treated mice, with 81.1 ± 17.7 per section, a 24% reduction from 106.1 ± 9.5 per section in the vehicle control–treated mice ($P = 0.046$, Kruskal–Wallis test). Representative H&E–stained sections can be seen in Supplementary Figure S3. These data indicate that inhibition of the Notch pathway using a γ-secretase inhibitor may be a potential therapeutic avenue for treatment of brain metastases from breast cancer.

To confirm and extend these trends, Notch1 silencing *via* shRNA was used to investigate the role of Notch1 in multiple facets of 231-BR cellular behavior. Notch1 shRNA reduced the expression of Notch1 mRNA, as determined by quantitative RT-PCR, in a specific manner (no reduction was observed for Notch2 to 4 mRNA levels) as shown on Figure 4A, and downstream transcriptional target Hey1 (Supplementary Fig. S2B). Notch1 knockdown resulted in a reduction in expression of CSC marker phenotype, from ∼90% to ∼70% of cells in the population exhibiting a $CD44^{hi}/CD24^{lo}$ expression pattern (with a concomitant change in the $CD44^{hi}/CD24^{hi}$ from ∼8.5% to ∼27%), suggesting a potential role for Notch1 in the maintenance of the CSC phenotype in 231-BR cells (Fig. 4B). *In vitro*, Notch1 shRNA resulted in a significant reduction in cellular growth at 24, 48, and 72 hours time points ($P = 0.033$, $P = 0.002$, $P = 0.009$, respectively; ANOVA; Fig. 4C). To ascertain *in vitro* aspects of the metastatic process, invasion assays were conducted using serum gradient as an attractant. An about 60% reduction in the ability of 231-BR cells to invade Matrigel was observed with Notch knockdown ($P < 0.001$, ANOVA; Fig. 4D).

The effect of Notch1 knockdown on formation of brain metastases was assessed by injecting nu/nu mice with 1.75×10^5 cells intracardiac, either 231-BR, 231-BR transiently transfected with scrambled shRNA or 231-BR transiently transfected with shNotch1. Metastases were allowed to colonize the brain for 28 days. At this time, brains were removed, formalin fixed, and paraffin embedded. Micro- and macrometastases were counted by 2 independent observers on H&E-stained sections (Table 2: representative stained sections can be seen in Supplementary Fig. S4). Cells transfected with shNotch1 formed an

Published OnlineFirst June 10, 2011; DOI: 10.1158/1541-7786.MCR-10-0457

Table 2. The effect of γ-secretase inhibition, using DAPT, and Notch1 silencing by shRNA, on the formation of brain metastases from 231-BR cells *in vivo*

Group	Incidence	Mean micrometastases (median: range)	Mean macrometastases (median: range)
γ-secretase inhibition			
Untreated	10/12	103.2 (101.5: 70–129)	34.6 (34: 22–52)
Vehicle control	9/12	106.1 (97.5: 65–166)	34.9 (35.5:21–48)
8 mg/kg DAPT	10/12	81.1 (85: 8–180)[a]	26.1 (20.5: 2–60)[a]
Notch1 silencing			
231-BR	7/8	91.7 (80: 22–173)	32.0 (30: 4–62)
231-BR-shScrambled	9/11	82.7 (84: 35–130)	23.6 (25: 9–38)
231-BR-shNotch1	7/12	17.4 (15: 3–49)[b]	5.8 (5: 1–18)[b]

NOTE: 1.75×10^5 cells were injected in nude mice via the intracardiac route. γ-Secretase inhibitor experiment: Metastases were allowed to form for 14 days prior to initiation of treatment. DAPT was administered i.p. on a 3-day on and 4-day off schedule, up to day 28 (total of 6 treatments). On day 28, mice were sacrificed and brains were removed for histological analysis. Numbers shown are an average of 3 sections per mouse (median value and range also displayed). Mice treated with DAPT developed significantly fewer metastases compared with vehicle-treated (5% ethanol in corn oil) or untreated mice. Data were analyzed using Kruskal–Wallis test. Notch silencing experiment: 1.75×10^5 cells (231-BR, 231-BR-shScrambled, and 231-BR-shNotch1) were injected in nude mice via the intracardiac route. Mice were sacrificed 28 days later and brains were removed for histological analysis. Cells transfected with shNotch1 formed significantly fewer micro- and macrometastases compared with untransfected cells or cells transfected with a scrambled sequence, when injected *in vivo*. Data were analyzed using Kruskal–Wallis test.

[a]$P < 0.05$.

[b]$P < 0.001$.

average of 5.8 ± 1.0 macrometastases per brain section, a 74% reduction as compared with cells expressing a scrambled shRNA (23.6 ± 1.5 per section) or untransfected 231-BR cells (32.6 ± 3.9 per section; $P < 0.001$; Kruskal–Wallis test). A similar reduction was observed in micrometastases using shRNA to Notch 1. Notch 1 shRNA transfected 231-BR cells produced a mean of 17.4 ± 2.9 micrometastases per section, a 79% decreased as compared with scrambled shRNA transfected 231-BR cells (82.7 ± 5.1 per section) or untransfected 231-BR cells (91.7 ± 9.9 per section; $P < 0.001$; Kruskal–Wallis test). These results extend the findings observed using γ-secretase inhibition, indicating a role for Notch signaling in the formation of brain metastases *in vivo*

Discussion

Brain metastasis from breast cancer has become the focus of recent investigations due to the inability of many current targeted therapies to effectively treat these tumors. Patients with brain metastases have very poor prognosis (2). Here we used an experimental model of breast cancer metastasis to brain, coupled with *in vitro* studies, to clarify mechanisms that can regulate brain metastasis. We have shown that a reduction in the proportion of CSC surface markers $CD44^{hi}/CD24^{lo}$ can give rise to the formation of significantly fewer brain metastases from breast cancer. This finding is in agreement with previous work by Croker and colleagues, who showed that breast cancer cells with a $CD44^{hi}/CD24^{lo}$ phenotype (albeit in addition to ALDH as a further tool for selection of the stem cell pool) displayed enhanced cell growth, colony formation, adhesion and invasion *in vitro*, and enhanced tumorigenicity and metastases formation in multiple organs in NOD/SCID-IL2Rγ null mice (13). In the results reported here, the $CD44^{lo}/CD24^{high}$ subpopulation retained a considerable amount of brain metastatic activity, however, suggesting that additional markers of "stemness" may be needed. In previous studies, $CD44^{hi}/CD24^{lo}$ cell subsets grown as mammospheres have been shown to be radioresistant, at DNA and cellular levels, compared with cells grown as a monolayer and the proportion of these breast cancer initiating cells increased following short courses of fractionated irradiation (47). It will be of interest to determine the radiosensitivity of these subpopulations as brain metastases are treated by both large doses (stereotactic radiation) and fractionated smaller doses (whole brain radiotherapy) of cranial irradiation.

The data presented herein provide a strong case for preclinical consideration of Notch signaling as a therapeutic target for brain metastases of breast cancer. Increased levels of cleaved Notch1 were detected in 231-BR cells, compared with parental 231 breast cancer cells, in agreement with results shown by Nam and colleagues who isolated a brain-metastatic derivative of the MDA-MB-435 cells, Br4 (40). The authors showed activation of the Notch pathway in the Br4 cells, including elevated levels of Jag2, Hes1, and Hey1 mRNA (40). Proliferative and migratory properties of these cells *in vitro* were significantly reduced

Published OnlineFirst June 10, 2011; DOI: 10.1158/1541-7786.MCR-10-0457

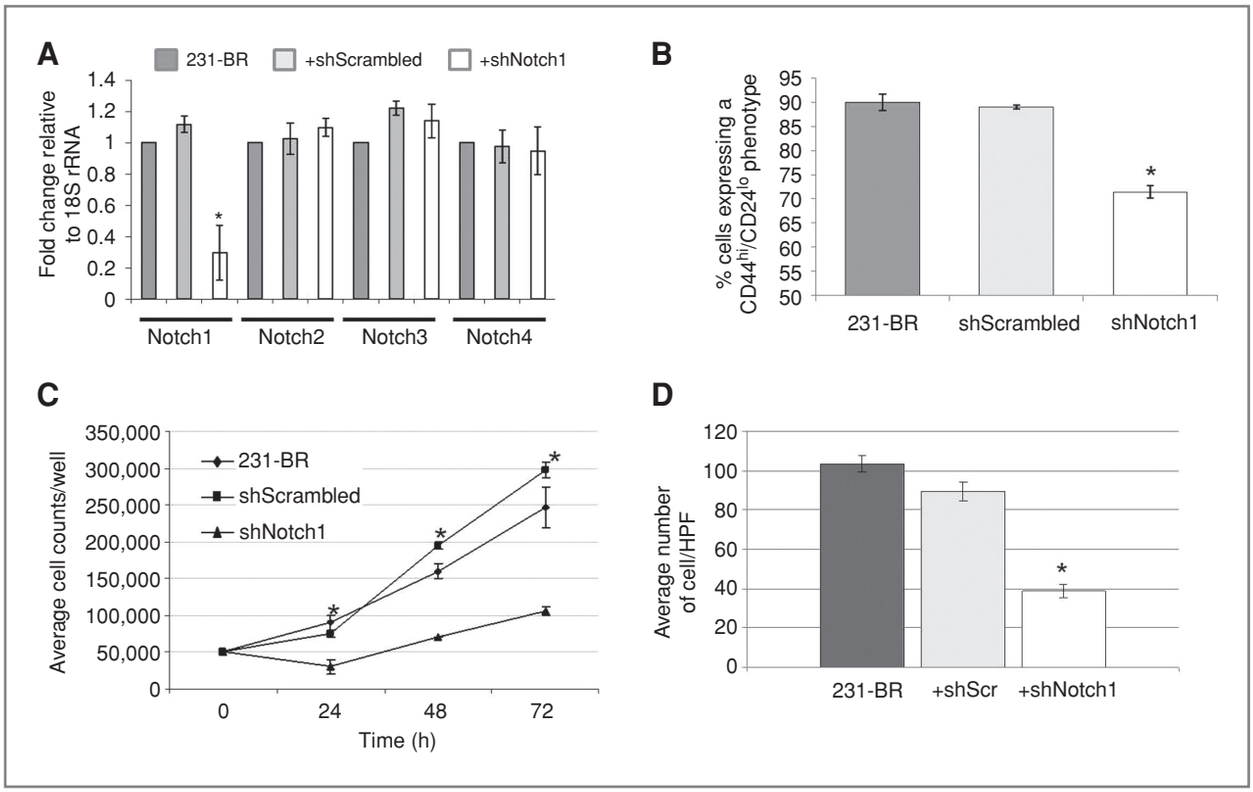

Figure 4. Effect of Notch1 silencing by shRNA on *in vitro* cellular behavior. A, Notch1 shRNA resulted in knockdown of Notch1 in a specific manner. No significant knockdown of Notch2, 3, or 4 was observed (*, $P < 0.05$; Student's paired *t* test shNotch1 compared with shScrambled). B, CSC markers, CD44 and CD24 were determined in 231-BR, 231-BR-shScrambled, and 231-BR-shNotch1 cells. Notch1 knockdown reduced the percentage of $CD44^{hi}/CD24^{lo}$ cells, compared with 231-BR and shScrambled control cells, by approximately 20% (*, $P < 0.05$, shNotch1 compared with shScrambled; Student's paired *t* test). C, Notch1 silencing resulted in a significant reduction in cellular growth at 24, 48, and 72 hours (*, $P = 0.033$, $P = 0.002$, $P = 0.009$, respectively, ANOVA). D, Notch1 knockdown significantly reduced the ability of 231-BR cells to invade through Matrigel, using 24-well transwell chambers (*, $P = 0.001$, ANOVA and $P < 0.05$ shNotch1 compared with shScrambled; Student's paired *t* test). Error bars: ± SEM.

upon treatment with DAPT or Notch1 RNAi (40). In addition, we found that inhibition of Notch1 *in vitro* resulted in decreased cell proliferation and invasion, similar to results found by Purow and colleagues and Rose and colleagues (48, 49) and reduced expression of Notch 1 to 4 mRNA. The effect of gamma secretase inhibition on Notch mRNA expression appears to be very cell-type and context dependent. In a recent publication, Wang and colleagues showed that DAPT reduced Notch mRNA levels in the ovarian cancer cell line A2870, in a dose-dependent manner (50). The authors treated ovarian cancer cells with varying doses of DAPT and found a reduction in Notch1 mRNA, as determined by RT-PCR (data normalized to beta-actin). In addition, the authors showed a significant reduction of Notch1 mRNA expression after 6 hours, which was sustained for up to 72 hours (50). The reason for this is unclear, though the regulation of Notch transcription remains largely unknown. Some studies have shown that DAPT treatment results in decreased NFκB nuclear translocation, reducing its activity (following LPS stimulation; ref 51). Reduction in NFκB has in turn been shown to reduce Notch1 mRNA transcript levels in melanocytes (52). A reduction in Notch1 mRNA levels in response to DAPT treatment was also observed, but this did not reach statistical significance (52).

Bos and colleagues identified a 243 gene signature in a genome wide expression analysis of parental CN34 and MDA-MB-231 breast cancer cells compared with derivatives that formed brain metastasis (53). Notch ligands, Jagged 1 and Jagged 2, were both identified as being differentially regulated in brain metastasis. This suggests, in agreement with the present study, that Notch signaling has a potential role in the formation of brain metastases from breast cancer. Similarly, Min and colleagues elucidated a panel of differentially regulated genes that may mediate breast cancer metastasis to the lung (54). Jagged 1 was also overexpressed in this study, which analyzed MDA-MB-231 and CM2 breast cancer cells selected for lung metastatic capability. However, in a gene panel of bone metastasis from breast cancer, Jagged 1 (or any Notch receptor or ligand) was not among the genes identified as potentially predicting metastasis to this site (55). It is clear that Notch signaling appears to be involved in many facets of tumor progression and may play a role in mediating metastasis not

Published OnlineFirst June 10, 2011; DOI: 10.1158/1541-7786.MCR-10-0457

only to the brain, but also to additional local and distant sites.

Two approaches were used to show that Notch signaling inhibition was causally linked to brain metastatic colonization in the 231-BR *in vivo* model system. First, administration of DAPT, beginning 14 days postinjection, resulted in about 25% reduction in the formation of both micro- and macrometastases. Knockdown of Notch 1 using shRNA resulted in a more complete inhibition of brain metastasis, 74% to 79%. The reasons for this discrepancy in efficacy may be numerous. First, using the shRNA approach, Notch 1 signaling was inhibited from the time of tumor cell injection into the circulation, while DAPT was only administered at a later time, when multiple micrometastases and a few macrometastases are generally visible. Though our transfections were transient, Notch1 was silenced for 7 days prior to Notch1 levels returning to baseline. As our stem-like population was also a dynamic one, we felt that this was an appropriate model for comparison.

It is possible that Notch signaling inhibition is more efficacious on single tumor cells or small micrometastases, and that clinical approaches should be aimed at prevention of brain metastases rather than their shrinkage, in line with data reported for vorinostat (56). Second, the brain permeability of DAPT is not known. Previous work using the 231-BR model system has established that brain metastases have heterogeneous levels of blood-brain barrier permeability (57), which could expose some lesions with suboptimal drug levels. In agreement with our study, a recent investigation showed that inhibition of Notch1 in primary breast tumor samples and cell lines reduced tumor formation *in vivo* and reduced stem cell activity ($ESA^+CD44^+CD24^{lo}$ phenotype), though they found that inhibition of Notch4 elicited a greater effect than inhibition of Notch1 in their models (58).

Taken together, our data indicate that Notch signaling plays an important role in the formation of brain metastases from breast cancer, in part due to its role in maintaining the pool of $CD44^{hi}/CD24^{lo}$ putative cancer "stem-like" cells. It remains to be determined whether the effects observed *vis-à-vis* CSCs and Notch inhibition are cell type, context and/or methodology dependent. Also, rational drug combinations using brain-permeable therapies and/or radiation will be a topic of further investigation. Currently, a clinical trial is underway in patients with advanced breast cancer using a Notch inhibitor (γ-secretase inhibitor), MK0752 (www.clinicaltrials.gov: NTC00106145). Results are anticipated in 2011. Further elucidation of the characteristics of these metastases may enable the development of novel therapeutic strategies for brain metastases from breast cancer.

Disclosure of Potential Conflicts of Interest

No potential conflicts of interest were disclosed.

Acknowledgments

The authors thank Dr. Kristin Chadwick (Robarts Research Institute, University of Western Ontario), for valuable advice and for conducting cell sort experiments, Dr. Dwayne Jackson (Department of Medical Biophysics, University of Western Ontario) for use of molecular facilities and Alysha Croker (Department of Anatomy & Cell Biology, University of Western Ontario) and Dr. Ben Hedley (London Laboratory Services Group, Hematology Research, London, Ontario) for help with flow cytometric analyses.

Grant Support

This research was supported by grant #W81XWH-06-2-0033 US Department of Defense Breast Cancer Research Program (A.F. Chambers, P.J. Foster, and P.S. Steeg). P.M. McGowan was the recipient of a Postdoctoral Fellowship from the Translational Breast Cancer Research Training Program at the London Regional Cancer Program. A.L. Allan is supported by research funding from the Ontario Institute of Cancer Research (#08NOV-230) and a Canadian Institutes of Health Research New Investigator Award. A.F. Chambers is Canada Research Chair in Oncology, supported by the Canada Research Chairs Program.

The costs of publication of this article were defrayed in part by the payment of page charges. This article must therefore be hereby marked *advertisement* in accordance with 18 U.S.C. Section 1734 solely to indicate this fact.

Received October 7, 2010; revised May 10, 2011; accepted May 11, 2011; published OnlineFirst June 10, 2011.

References

1. Weil RJ, Palmieri DC, Bronder JL, Stark AM, Steeg PS. Breast cancer metastasis to the central nervous system. Am J Pathol 2005;167:913–20.
2. Palmieri D, Smith QR, Lockman PR, Bronder J, Gril B, Chambers AF, et al. Brain metastases of breast cancer. Breast Dis 2006;26:139–47.
3. Gaedcke J, Traub F, Milde S, Wilkens L, Stan A, Ostertag H, et al. Predominance of the basal type and HER-2/neu type in brain metastasis from breast cancer. Mod Pathol 2007;20:864–70.
4. Lower EE, Drosick DR, Blau R, Brennan L, Danneman W, Hawley DK. Increased rate of brain metastasis with trastuzumab therapy not associated with impaired survival. Clin Breast Cancer 2003;4:114–9.
5. Lin NU, Bellon JR, Winer EP. CNS metastases in breast cancer. J Clin Oncol 2004;22:3608–17.
6. Lin NU, Winer EP. Brain metastases: the HER2 paradigm. Clin Cancer Res 2007;13:1648–55.
7. Steeg PS, Camphausen KA, Smith QR. Brain metastases as preventive and therapeutic targets. Nat Rev Cancer 2011;11:352–63.
8. Clarke MF. Oncogenes, self-renewal and cancer. Pathol Biol 2006; 54:109–11.
9. Al-Hajj M, Wicha MS, Benito-Hernandez A, Morrison SJ, Clarke MF. Prospective identification of tumorigenic breast cancer cells. Proc Natl Acad Sci USA 2003;100:3983–8.
10. Hess DA, Meyerrose TE, Wirthlin L, Craft TP, Herrbrich PE, Creer MH, et al. Functional characterization of highly purified human hematopoietic repopulating cells isolated according to aldehyde dehydrogenase activity. Blood 2004;104:1648–55.
11. Hess DA, Wirthlin L, Craft TP, Herrbrich PE, Hohm SA, Lahey R, et al. Selection based on CD133 and high aldehyde dehydrogenase activity isolates long-term reconstituting human hematopoietic stem cells. Blood 2006;107:2162–9.
12. Ginestier C, Hur MH, Charafe-Jauffret E, Monville F, Dutcher J, Brown M, et al. ALDH1 is a marker of normal and malignant human mammary stem cells and a predictor of poor clinical outcome. Cell Stem Cell 2007;1:555–67.
13. Croker AK, Goodale D, Chu J, Postenka C, Hedley BD, Hess DA, et al. High aldehyde dehydrogenase and expression of cancer stem cell markers selects for breast cancer cells with enhanced malignant and metastatic ability. J Cell Mol Med 2009; 13:2236–52.
14. Hartmann D, de Strooper B, Serneels L, Craessaerts K, Herreman A, Annaert W, et al. The disintegrin/metalloprotease ADAM 10 is essential for Notch signalling but not for alpha-secretase activity in fibroblasts. Hum Mol Genet 2002;11:2615–24.

Published OnlineFirst June 10, 2011; DOI: 10.1158/1541-7786.MCR-10-0457

15. Brou C, Logeat F, Gupta N, Bessia C, LeBail O, Doedens JR, et al. A novel proteolytic cleavage involved in Notch signaling: the role of the disintegrin-metalloprotease TACE. Mol Cell 2000;5:207–16.
16. Ray WJ, Yao M, Mumm J, Schroeter EH, Saftig P, Wolfe M, et al. Cell surface presenilin-1 participates in the gamma-secretase-like proteolysis of Notch. J Biol Chem 1999;274:36801–7.
17. Chen Y, Fischer WH, Gill GN. Regulation of the ERBB-2 promoter by RBPJkappa and NOTCH. J Biol Chem 1997;272:14110–4.
18. Ronchini C, Capobianco AJ. Induction of cyclin D1 transcription and CDK2 activity by Notch(ic): implication for cell cycle disruption in transformation by Notch(ic). Mol Cell Biol 2001;21:5925–34.
19. Suzuki T, Aoki D, Susumu N, Udagawa Y, Nozawa S. Imbalanced expression of TAN-1 and human Notch4 in endometrial cancers. Int J Oncol 2000;17:1131–9.
20. Veenendaal LM, Kranenburg O, Smakman N, Klomp A, Borel Rinkes IH, van Diest PJ. Differential Notch and TGFbeta signaling in primary colorectal tumors and their corresponding metastases. Cell Oncol 2008;30:1–11.
21. Dang TP, Gazdar AF, Virmani AK, Sepetavec T, Hande KR, Minna JD, et al. Chromosome 19 translocation, overexpression of Notch3, and human lung cancer. J Natl Cancer Inst 2000;92:1355–7.
22. Stylianou S, Clarke RB, Brennan K. Aberrant activation of notch signaling in human breast cancer. Cancer Res 2006;66:1517–25.
23. Mungamuri SK, Yang X, Thor AD, Somasundaram K. Survival signaling by Notch1: mammalian target of rapamycin (mTOR)-dependent inhibition of p53. Cancer Res 2006;66:4715–24.
24. Lee CW, Simin K, Liu Q, Plescia J, Guha M, Khan A, et al. A functional Notch-survivin gene signature in basal breast cancer. Breast Cancer Res 2008;10:R97.
25. Dickson BC, Mulligan AM, Zhang H, Lockwood G, O'Malley FP, Egan SE, et al. High-level JAG1 mRNA and protein predict poor outcome in breast cancer. Mod Pathol 2007;20:685–93.
26. Dontu G, Jackson KW, McNicholas E, Kawamura MJ, Abdallah WM, Wicha MS. Role of Notch signaling in cell-fate determination of human mammary stem/progenitor cells. Breast Cancer Res 2004;6:R605–15.
27. Bouras T, Pal B, Vaillant F, Harburg G, Asselin-Labat ML, Oakes SR, et al. Notch signaling regulates mammary stem cell function and luminal cell-fate commitment. Cell Stem Cell 2008;3:429–41.
28. Bolos V, Blanco M, Medina V, Aparicio G, Diaz-Prado S, Grande E. Notch signalling in cancer stem cells. Clin Transl Oncol 2009;11:11–9.
29. Pannuti A, Foreman K, Rizzo P, Osipo C, Golde T, Osborne B, et al. Targeting Notch to target cancer stem cells. Clin Cancer Res 2010;16:3141–52.
30. Kakarala M, Wicha MS. Cancer stem cells: implications for cancer treatment and prevention. Cancer J 2007;13:271–5.
31. Farnie G, Clarke RB. Mammary stem cells and breast cancer—role of Notch signalling. Stem Cell Rev 2007;3:169–75.
32. Grudzien P, Lo S, Albain KS, Robinson P, Rajan P, Strack PR, et al. Inhibition of Notch signaling reduces the stem-like population of breast cancer cells and prevents mammosphere formation. Anticancer Res 2010;30:3853–67.
33. Monteiro J, Fodde R. Cancer stemness and metastasis: Therapeutic consequences and perspectives. Eur J Cancer 2010;46:1198–203.
34. Charafe-Jauffret E, Ginestier C, Iovino F, Wicinski J, Cervera N, Finetti P, et al. Breast cancer cell lines contain functional cancer stem cells with metastatic capacity and a distinct molecular signature. Cancer Res 2009;69:1302–13.
35. van den Hoogen C, van der Horst G, Cheung H, Buijs JT, Lippitt JM, Guzmán-Ramírez N, et al. High aldehyde dehydrogenase activity identifies tumor-initiating and metastasis-initiating cells in human prostate cancer. Cancer Res 2010;70:5163–73.
36. Hughes D. How the NOTCH pathway contributes to the ability of osteosarcoma cells to metastasize. Cancer Treat Res 2010;152:479–96.
37. Chen J, Imanaka N, Chen J, Griffin J. Hypoxia potentiates Notch signaling in breast cancer leading to decreased E-cadherin expression and increased cell migration and invasion. Br J Cancer 2010;102:351–60.
38. Hafeez BB, Adhami V, Asim M, Siddiqui IA, Bhat KM, Zhong W, et al. Targeted knockdown of Notch1 inhibits invasion of human prostate cancer cells concomittant with inhibition of matrix metalloproteinase-9 and urokinase plasminogen activator. Clin Cancer Res 2009;15:452–9.
39. Hu X, Feng F, Wang Y, Wang L, He F, Dou GR, et al. Blockade of Notch signaling in tumor-bearing mice may lead to tumor regression, progression or metastasis, depending on tumor cell types. Neoplasia 2009;11:32–8.
40. Nam D, Jeon H, Kim S, Kim MH, Lee YJ, Lee MS, et al. Activation of Notch signaling in a xenograft model of brain metastasis. Clin Cancer Res 2008;14:4059–66.
41. Yoneda T, Williams PJ, Hiraga T, Niewolna M, Nishimura R. A bone-seeking clone exhibits different biological properties from the MDA-MB-231 parental human breast cancer cells and a brain-seeking clone in vivo and in vitro. J Bone Miner Res 2001;16:1486–95.
42. Gril B, Palmieri D, Bronder JL, Herring JM, Vega-Valle E, Feigenbaum L, et al. Effect of lapatinib on the outgrowth of metastatic breast cancer cells to the brain. J Natl Cancer Inst 2008;100:1092–103.
43. Sjölund J, Johansson M, Manna S, Norin C, Pietras A, Beckman S, et al. Suppression of renal cell carcinoma growth by inhibition of Notch signaling in vitro and in vivo. J Clin Invest 2008;118:217–28.
44. van Es JH, van Gijn ME, Riccio O, van den Born M, Vooijs M, Begthel H, et al. Notch/gamma-secretase inhibition turns proliferative cells in intestinal crypts and adenomas into goblet cells. Nature 2005;435:959–63.
45. Pfaffl MW. A new mathematical model for relative quantification in real time RT-PCR. Nucleic Acids Res 2001;29:e45.
46. van de Vijver MJ, He YD, van't Veer LJ, Dai H, Hart AA, Voskuil DW, et al. A gene-expression signature as a predictor of survival in breast cancer. N Engl J Med 2002;347:1999–2009.
47. Phillips TM, McBride WH, Pajonk F. The response of CD24(−/low)/CD44 +breast cancer-initiating cells to radiation. J Natl Cancer Inst 2006;98:1777–85.
48. Purow BW, Haque RM, Noel MW, Su Q, Burdick MJ, Lee J, et al. Expression of Notch-1 and its ligands, delta-like-1 and jagged-1, is critical for glioma cell survival and proliferation. Cancer Res 2005;65:2353–63.
49. Rose SL, Kunnimalaiyaan M, Drenzek J, Seiler N. Notch 1 signaling is active in ovarian cancer. Gynecol Oncol 2010;117:130–3.
50. Wang M, Wu L, Wang L, Xin X. Downregulation of Notch1 by gamma secretase inhibition contributes to cell growth inhibition and apoptosis in ovarian cancer cells A2780. Biochem Biophys Res Commun 2010;393:144–9.
51. Monsalve E, Ruiz-García A, Baladrón V, Ruiz-Hidalgo MJ, Sánchez-Solana B, Rivero S, et al. Notch1 upregulates LPS-induced macrophage activation by increasing NF-kappaB activity. Eur J Immunol 2009;39:2556–70.
52. Bedogni B, Warneke JA, Nickoloff BJ, Giaccia AJ, Powell MB. Notch1 is an effector of Akt and hypoxia in melanoma development. J Clin Invest 2008;118:3660–70.
53. Bos PD, Zhang XH, Nadal C, Shu W, Gomis RR, Nguyen DX, et al. Genes that mediate breast cancer metastasis to the brain. Nature 2009;459:1005–9.
54. Minn AJ, Gupta GP, Siegel PM, Bos PD, Shu W, Giri DD, et al. Genes that mediate breast cancer metastasis to lung. Nature 2005;436:518–24.
55. Smid M, Wang Y, Klijn JG, Sieuwerts AM, Zhang Y, Atkins D, et al. Genes associated with breast cancer metastatic to bone. J Clin Oncol 2006;24:2261–7.
56. Palmieri D, Lockman P, Thomas F, Hua E, Herring J, Hargrave E, et al. Vorinostat inhibits brain metastatic colonization in a model of triple-negative breast cancer. Clin Cancer Res 2009;15:6148–57.
57. Lockman PR, Mittapalli RK, Taskar KS, Rudraraju V, Gril B, Bohn KA, et al. Heterogeneous blood-tumor barrier permeability determines drug efficacy in experimental brain metastases of breast cancer. Clin Cancer Res 2010;16:5664–78.
58. Harrison H, Farnie G, Howell SJ, Rock RE, Stylianou S, Brennan KR, et al. Regulation of breast cancer stem cell activity by signaling through the Notch4 receptor. Cancer Res 2010;70:709–18.

Published OnlineFirst June 10, 2011; DOI: 10.1158/1541-7786.MCR-10-0457

Molecular Cancer Research

Notch1 Inhibition Alters the CD44^{hi}/CD24^{lo} Population and Reduces the Formation of Brain Metastases from Breast Cancer

Patricia M. McGowan, Carmen Simedrea, Emeline J. Ribot, et al.

Mol Cancer Res 2011;9:834-844. Published OnlineFirst June 10, 2011.